# Experimental and Simulation Evidence of a Corkscrew Motion for Benzene in the Metal–Organic Framework MIL-47

**ARTICLE** *in* THE JOURNAL OF PHYSICAL CHEMISTRY C · JULY 2012

Impact Factor: 4.77 · DOI: 10.1021/jp302995b



**8 AUTHORS**, INCLUDING:

Daniil Kolokolov
Boreskov Institute of Catalysis
**28** PUBLICATIONS **293** CITATIONS
SEE PROFILE

Alexander G Stepanov
Boreskov Institute of Catalysis
**135** PUBLICATIONS **1,658** CITATIONS
SEE PROFILE

Jacques Ollivier
Institut Laue-Langevin
**121** PUBLICATIONS **995** CITATIONS
SEE PROFILE

Guillaume Maurin
Université de Montpellier
**217** PUBLICATIONS **6,543** CITATIONS
SEE PROFILE

THE JOURNAL OF PHYSICAL CHEMISTRY C

Article

pubs.acs.org/JPCC

# Experimental and Simulation Evidence of a Corkscrew Motion for Benzene in the Metal–Organic Framework MIL-47

Daniil I. Kolokolov,[†,‡] Hervé Jobic,*[,†] Alexander G. Stepanov,[‡] Jacques Ollivier,[§] Sébastien Rives,[†,∥] Guillaume Maurin,[∥] Thomas Devic,[⊥] Christian Serre,[⊥] and Gérard Férey[⊥]

[†]Institut de Recherches sur la Catalyse et l'Environnement de Lyon, UMR CNRS 5256, Université Lyon 1, 2. Av. A. Einstein, 69626 Villeurbanne, France

[‡]Boreskov Institute of Catalysis, Siberian Branch of Russian Academy of Sciences, Prospekt Akademika Lavrentieva 5, Novosibirsk 630090, Russia

[§]Institut Laue Langevin, BP 156, 38042 Grenoble, France

[∥]Institut Charles Gerhardt Montpellier, UMR CNRS 5253, ENSCM, Place E. Bataillon, 34095 Montpellier, France

[⊥]Institut Lavoisier, UMR CNRS 8180, Université de Versailles Saint-Quentin-en-Yvelines, 78035 Versailles, France

Supporting Information

**ABSTRACT:** Some bacteria move with a corkscrew motion, meeting less resistance from surrounding water. A spiral movement is also considered during RNA polymerase translocation and it has been observed for water and proteins. We have found that benzene molecules confined in the metal–organic framework MIL-47 move in a corkscrew fashion. This spectacular diffusion effect could be put into evidence by combining experimental and computation tools; the two experimental techniques, quasielastic neutron scattering and $^2$H NMR, cover a wide range of time scales.

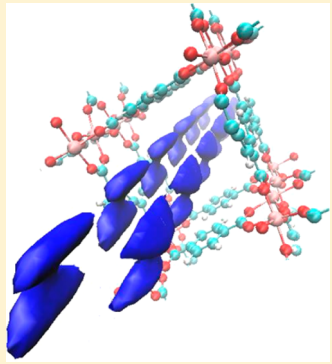

## 1. INTRODUCTION

Most of the macroscopic properties of interfaces have their origin at the molecular level. The dynamics of guest molecules within a host matrix is thus the cornerstone of any sorbent/sorbate system, and it represents a matter of both practical and fundamental interest. Recently, a new type of porous material, a metal–organic framework (MOF), was envisaged as a possible effective medium in hydrocarbon separation processes; particularly promising performances were reported concerning aromatic molecules separation (xylenes, benzene, cyclohexane) on the MOF-type MIL-47(V).[1−4] MOFs belong to an emerging class of coordination polymers built from metal oxide nodes connected together by bridging organic "linkers".[5−7] In the case of MIL-47(V), the framework consists of infinite chains of corner-sharing $V^{4+}O_6$ octahedra interconnected by 1,4-benzenedicarboxylate groups, creating a 3D framework of 1D channels about 8 Å in free diameter.[8] As a preliminary step to improve our understanding of the separation mechanism of aromatics in MIL-47(V), the simplest aromatic compound, benzene, is an ideal candidate to investigate the peculiarities of its dynamic behavior at the molecular level.

Although the dynamics of benzene in zeolites has been studied by a variety of experimental and computational methods,[9−12] only a few works regarding benzene in MOFs were published so far. The mobility of benzene was first explored in MOF-5 using $^2$H NMR and Monte Carlo techniques[13] and later by PFG NMR[14] and molecular dynamics (MD) simulations.[15] Recently, the adsorption of benzene in MIL-47(V) was followed by pulse chromatography and Monte Carlo simulations.[16]

In the present work, we characterize the dynamics of benzene entrapped in the MIL-47(V) host matrix by quasielastic neutron scattering (QENS) and solid-state $^2$H NMR, combined with molecular simulations. Excellent agreement has been obtained in recent years between QENS and molecular simulations on the quantitative study of molecular motion of pure and mixed fluids sorbed in zeolites and MOFs.[17] One of the reasons is that both methods operate over the same time and length scales. The QENS technique provides detailed information not only on translational diffusion, but also on local motions such as rotation. The conclusions drawn from the simulations can thus be tested by QENS at a truly microscopic level. However, if rotational motions occur on longer time scales, the $^2$H NMR technique is better suited than the QENS method.

**Received:** March 29, 2012
**Revised:** June 28, 2012
**Published:** June 28, 2012

  

## 2. EXPERIMENTAL SECTION

**2.1. Materials.** Synthesis and activation of MIL-47(V) were performed using published procedures[8] with hydrogenated or deuterated terephthalic acid as a reactant for the NMR or QENS experiments, respectively.

**2.2. Neutron Scattering.** The QENS measurements were performed on the time-of-flight (TOF) spectrometer IN5, at the Institut Laue-Langevin. The incident wavelength was taken as 8 Å, corresponding to a neutron energy of 1.28 meV. The elastic energy resolution, measured with a vanadium standard, corresponds to a Gaussian function, with a half-width at half-maximum (HWHM) close to 11 $\mu$eV. The scattered neutrons were analyzed as a function of flight-time and angle. The TOF of the scattered neutrons is related to the energy transfer ($\hbar\omega$) and the scattering angle to the wave-vector transfer ($Q$). The TOF spectra were transformed to an energy scale after subtracting the scattering of the empty MOF. Groupings of detectors were made at various $Q$ values, avoiding the Bragg peaks of MIL-47(V). The adsorption of benzene resulted in slight shifts of the Bragg peaks, as shown in Figure 1, indicating that the structure is not totally rigid.

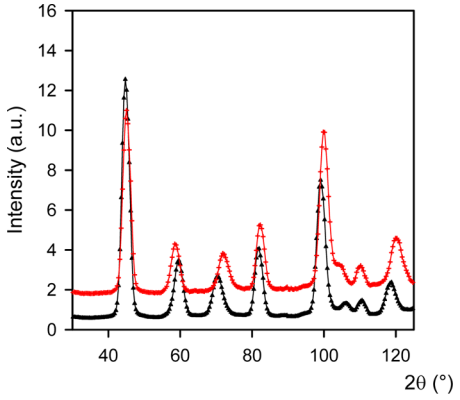


**Figure 1.** Neutron diffraction patterns of MIL-47(V) empty (black triangle) and of MIL-47(V) with one molecule of benzene per unit cell (red plus) ($T$ = 300 K, $\lambda$ = 8 Å). The patterns were obtained by comparing the elastic peak intensities, at each angular position, with those obtained from a vanadium standard. Since benzene is totally hydrogenated, its effect on the neutron diffraction pattern is reflected in a background increase.

MIL-47(V) was degassed at 473 K, under a vacuum of $10^{-5}$ Torr (1 Torr = 133.3 Pa). Two samples were then prepared and transferred inside a glovebox into slab-shaped aluminum containers. For the first sample, a known amount of benzene, corresponding to 1 molecule per unit cell (uc), was adsorbed onto the MOF and equilibrated at 373 K. The second cell contained degassed MIL-47(V), with a weight identical to that of the first sample, 1.2 g.

**2.3. NMR Measurements.** $^2$H NMR experiments were performed at 61.432 MHz on a Bruker Avance-400 spectrometer, using a high power probe with 5 mm horizontal solenoid coil. Metallic centers in the MIL-47(V) structure are paramagnetic ($V^{4+}$, $S = {}^1/_2$) which may influence the $^2$H NMR spectrum by large frequency shifts and fast relaxation of the nuclear spin.[18] To compensate these effects and correctly refocus the $^2$H NMR spectrum an exorcycled quadrupole-echo sequence was used,[19] $(90_X-\tau_1-90_Y-\tau_2-\text{Acq}-t)$, where $\tau_1 = 20\ \mu$s, $\tau_2 = 22\ \mu$s, and $t$ is a repetition time for the sequence during the accumulation of the NMR signal. The duration of the 90° pulses was 3.0−3.2 $\mu$s. To capture all dynamical features of the system, the measurements were performed over a broad temperature range, from 123 to 403 K. Perdeuterated benzene-$d_6$ with 98% $^2$H isotopic enrichment was purchased from Cambridge Isotope Laboratories Inc. and used without further purification.

To prepare the sample, 0.3 g of MIL-47(V) was loaded in a 5 mm (o.d.) glass tube, connected to a vacuum system. The sample was heated at 473 K for 12 h in air and for 24 h under a vacuum of $10^{-5}$ Torr. After cooling back to room temperature, the material was loaded with 1 molecule of benzene per uc and sealed off. The adsorption was performed from the gas phase with the MOF powder kept at the temperature of liquid nitrogen. The sealed sample was equilibrated at 373 K for 10 h.

**2.4. Computational Methodology.** The periodic model of the MIL-47(V) framework was built using the coordinates of the atoms previously reported.[8] The framework was maintained rigid during the simulations, this assumption being justified by the small change of the MIL-47(V) structure in the presence of benzene, as evidenced by neutron diffraction (Figure 1). The partial charges carried by each atom were taken from our previous DFT calculations.[20] The inorganic node of MIL-47(V) (corresponding to the metal center with the surrounding oxygen atoms) was described by the UFF force field,[21] whereas the organic part was treated using the Dreiding force field.[22] The benzene guest molecule was treated using the explicit TraPPE-EH rigid charged model.[23] For the interactions between benzene and each atom of the framework, interatomic potential parameters were obtained using Lorentz−Berthelot mixing rules. MD simulations were realized using the DL_POLY package[24] in the *NVT* ensemble coupled with either the Beredsen or Nosé−Hoover thermostat.[25] The simulation box consisted of 32 unit cells loaded by 32 benzene molecules to be consistent with the experimental loading. The calculations were run at three different temperatures, each for $10^7$ steps (i.e., 10 ns in total) with a time step of 1 fs, following 1 ns of equilibration. From the mean square displacement (MSD) curves averaged over multiple time origins and five different MD trajectories, the self-diffusivities ($D_s$) for benzene were evaluated based on the Einstein equation.[25] The rotational diffusivity about the $C_2$ and $C_6$ axis was estimated from the angular velocity autocorrelation function.[25] The 2D free-energy maps and isosurfaces were then obtained using the histogram sampling method previously reported by Beerdsen et al.[26]

## 3. RESULTS AND DISCUSSION

Since the interpretation of the QENS data is generally simpler than in solid-state $^2$H NMR, these results were analyzed first. To follow the molecular motions of adsorbed benzene by QENS, the hydrogenated molecule was used because of the large incoherent cross section of hydrogen. On the other hand, the framework was deuterated, to decrease the scattering from the organic linkers. Experimental QENS spectra, obtained after subtraction of the empty framework contribution, are shown in Figure 2. The measured intensities are presented in terms of the dynamical structure factor, $S(Q,\omega)$, where $\hbar Q$ and $\hbar\omega$ are the momentum and energy transfers, respectively. Schematically, one can differentiate two components in the spectra: a narrow one that is broader than the instrumental resolution because of the translational motion of benzene and a broad one that is essentially due to the rotation of the molecule.

The measured intensities are proportional to a scattering function that is the convolution product of the translational and


dx.doi.org/10.1021/jp302995b | J. Phys. Chem. C 2012, 116, 15093−15098

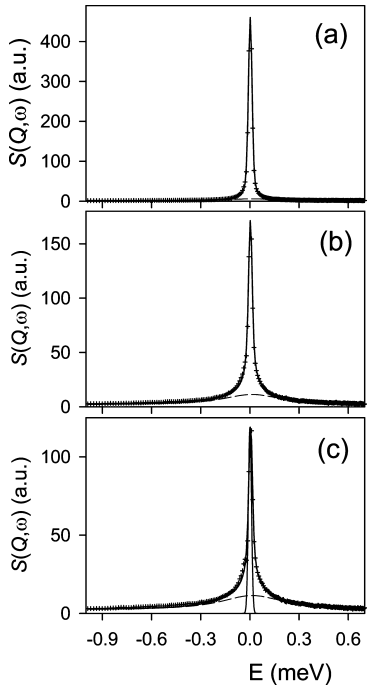


**Figure 2.** Comparison between experimental and calculated QENS spectra obtained for benzene in MIL-47(V) at 370 K, for different $Q$ values: (a) 0.21 Å$^{-1}$, (b) 0.44 Å$^{-1}$, and (c) 0.51 Å$^{-1}$. The crosses correspond to the experimental points and the solid lines to the calculated spectra, and the dashed lines indicate the contribution from rotation. The narrow elastic peak in part c corresponds to the instrumental resolution.

rotational motions. For the rotation, a uniaxial rotation about the $C_6$ axis, consisting of jumps of $2\pi/6$, could reproduce the broad quasielastic component in Figure 2. For this model,[27] the radius of gyration converged to 2.5 Å, at the different temperatures. An isotropic rotational model could not fit properly the spectra. The $C_6$ rotation is the fastest motion, it occurs on the ps time scale and its activation energy is of 2.9 kJ/mol.

The other molecular motion that is observed by QENS is a translation along the channels. Fits of the QENS spectra showed that a one-dimensional diffusion matched better the experimental data than a three-dimensional diffusion, at all temperatures. The finding that the QENS spectra could be fitted by a normal 1D diffusion indicates that the benzene molecules are able to pass each other in the MIL-47(V) channels; i.e., no single-file diffusion is observed.

The self-diffusion coefficients were derived from the broadenings, due to the translation of the molecule, as a function of wave-vector transfer.[17] The HWHMs of the translational scattering functions are plotted in Figure 3 as a function of $Q^2$. The experimental points deviate from straight lines at the different temperatures. A linear variation of the HWHM is obtained for Fickian diffusion when continuous diffusion takes place.[17] For benzene in MIL-47(V), one observes a deviation from a linear relation at large $Q$, which is a signature of jump diffusion.

All spectra could be fitted simultaneously using a jump diffusion model with a distribution of jump lengths.[28] The excellent agreement between experimental and calculated QENS spectra is shown in Figure 2. The mean jump length for benzene is 3.5 Å at 300 K. The technique thus probes a length scale ranging from the elementary jumps such as the ones displayed in

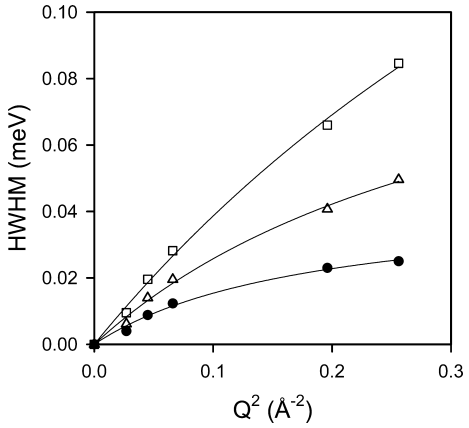


**Figure 3.** Half-width at half-maximum versus $Q^2$ of the translational component in the spectra of benzene in MIL-47(V) at different temperatures: (●) 300 K, (△) 330 K, and (□) 370 K. The different points were obtained from individual fits of the spectra and the solid lines with simultaneous fits with a jump diffusion model.

Figure 4, to a few unit cells over which a diffusion coefficient can be derived.

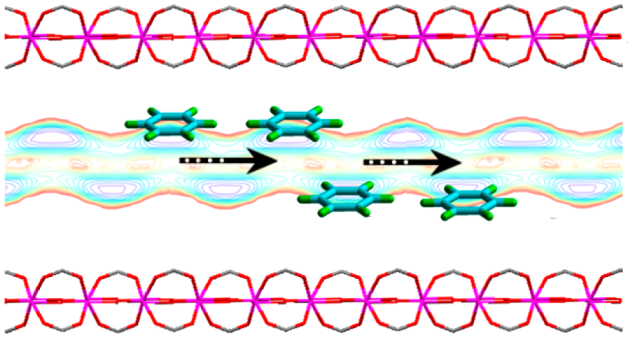

**Figure 4.** Benzene inside MIL-47(V) moves along the channels axis by short length jumps.

The self-diffusion coefficients, which are reported in Figure 5, are orientationally averaged values ($D_s = D_{1D}/3$). The activation energy obtained from this Arrhenius representation is 8 kJ/mol.

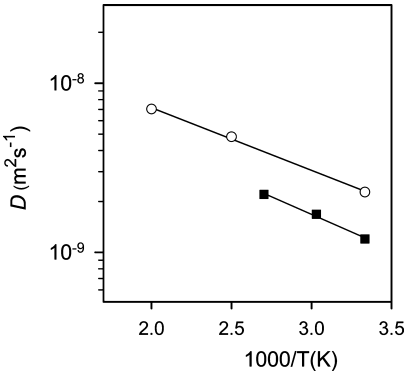


**Figure 5.** Self-diffusion coefficients ($D_s$) for benzene in MIL-47(V) as a function of temperature: QENS (full symbols) and MD (empty symbols).

To get additional microscopic insight into the diffusion mechanism in play, MD simulations were conducted for benzene


dx.doi.org/10.1021/jp302995b | J. Phys. Chem. C 2012, 116, 15093−15098

loading and temperatures that mimic the experimental conditions. From these MD runs, free-energy isosurfaces were derived from spatial density probabilities, while the trajectories followed by the benzene molecule were carefully analyzed. From the free-energy isosurfaces corresponding to the most probable spatial probabilities (Figure 6a), four distinct lower energy regions are evidenced; they are labeled A1, A2, B1, and B2 in Figure 6b–d. One obtains an unusual periodical distribution of zones forming a spiral inside the channel. Benzene is expected to travel along a minimum energy pathway involving jump sequences between these regions.

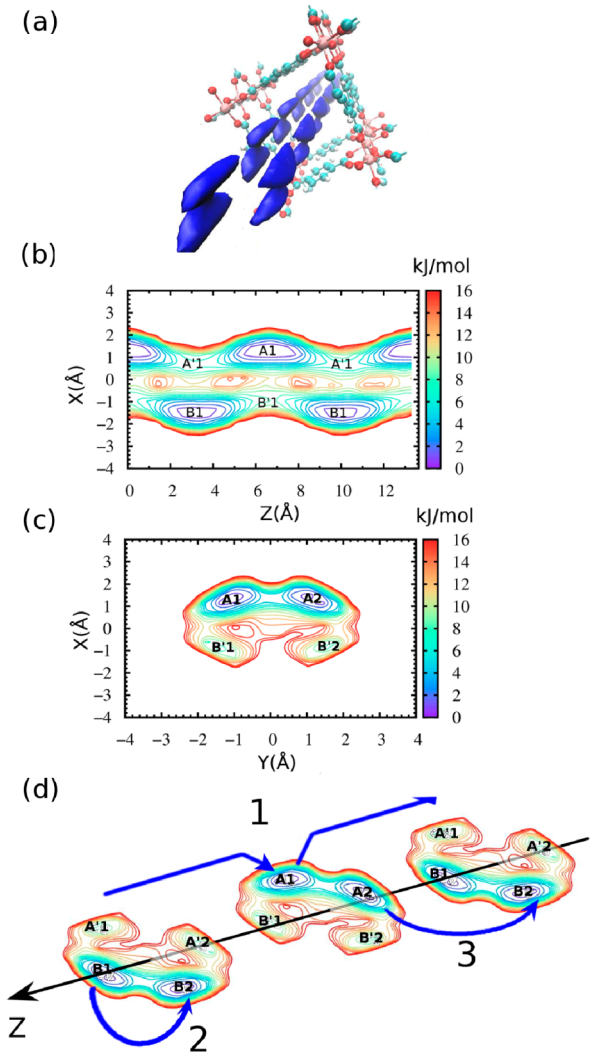


**Figure 6.** (a) Free energy isosurface at 5 kJ/mol showing low-energy regions for benzene in MIL-47(V) along a 2-fold screw axis. (b) 2D slice of the free-energy map along the channel direction, the isolines spacing being 1 kJ/mol; A1 and B1 are free-energy pockets, while A′1 and B′1 are barriers. (c) 2D slice of the free-energy map through the channel plane (isolines spacing of 1 kJ/mol); A1 and A2 are free-energy pockets while B′1 and B′2 are barriers. (d) Representation of the three main jumps for benzene within a channel of MIL-47(V); the arrows indicate the displacements of the center of mass of the molecule.

Within these zones, the centers of mass of benzene are located at a mean distance of 1.8 Å from the center of the channel, and the molecules are preferentially oriented with their $C_6$-axis perpendicular to the tunnel, with four possible orientations in the channel plane separated by 90°. From the free-energy isosurfaces combined with the MD trajectories, one can distinguish three main jumps, each associated with a specific activation barrier:

(i) a translational motion along the tunnel by jumps between sites located at similar *x,y* positions within a channel (i.e., A1 → A′1 → A1), with the molecule gliding with its $C_2$-axis parallel to the tunnel (jump 1 in Figure 6d); this displacement requires crossing an energy barrier of 7–8 kJ/mol;

(ii) a jump exchange between two positions in the same *x,y* plane, i.e. A1 → A2 or B1 → B2 jumps, as shown by the arrow 2 in Figure 6d; the energy barrier for this motion is 5–6 kJ/mol;

(iii) a transversal jump between sites A1 → B1 or A2 → B2 (jump 3 in Figure 6d); this latter motion is characterized by a higher energy barrier of 12 kJ/mol and it includes both a change of position in the channel plane *x,y* and along the channels axis *z*.

These MD trajectories were further used to compute the self-diffusivity of benzene. The simulated $D_s$ values are presented in Figure 5, the activation barrier being 7.1 kJ/mol. The body-fixed translational self-diffusion along the $C_2$ or $C_6$-axes extracted from velocity autocorrelation functions shows that the benzene molecule glides mainly along one of its $C_2$-axes. This indicates that on a length scale of a few unit cells, the diffusion is mainly governed by the first type of jumps, i.e. A1 → A′1 → A1, with the benzene molecule moving along the channel axis. Furthermore, MD simulations evidence a fast rotational dynamics around the $C_6$-axis with an activation energy of 2.7 kJ/mol. This shows that the MD description of the translational and $C_6$ rotational motions of benzene agrees very well with the QENS measurements.

The analysis of the MD trajectories responsible for the second and third main jumps evidences that these motions have more degrees of freedom: normally most of the molecules have their $C_2$ axis along the channel axis and this is preserved during the jumps. However, there are two types of events in which the orientation of the molecule changes: the first and most frequent (≈1% of all jumps) combines a translation in the *x,y* plane with a $\pi/2$-rotation of the benzene molecule around its $C_2$-axis parallel to the channel axis. The second one, less frequent (≈0.1% of all jumps), changes the orientation of the molecule during a jump in such a way that in the final position the molecule stands with its plane perpendicular to the channel axis.

The rates estimated for the events involving a reorientation of the molecular plane with respect to the channel axis are too slow to be detected by the QENS technique (time scales longer than $10^{-10}$ s are not accessible during our experiment). Further, the third main jump runs into the same situation because of its higher activation barrier.

Hence, to experimentally evidence the presence of these unusual motions, a technique capable of monitoring slower rotations is needed. This is why $^2$H NMR was applied. The experimental results (Figure 7a) show that below 163 K, the $^2$H NMR spectra line shape is characterized by a symmetric Pake powder pattern with a quadrupolar constant of $Q_1 \approx 93$ kHz;[29] thus, at low temperatures benzene is involved solely in the uniaxial rotation around the $C_6$ symmetry axis.

Above 163 K, the line shape starts to change in a remarkable manner, showing a progressive increase of two additional signals: a new anisotropic one with a smaller effective interaction constant of $Q_2 \approx 47$ kHz and the isotropic one, located at the center of the spectrum. With the temperature evolution, both


dx.doi.org/10.1021/jp302995b | J. Phys. Chem. C 2012, 116, 15093–15098

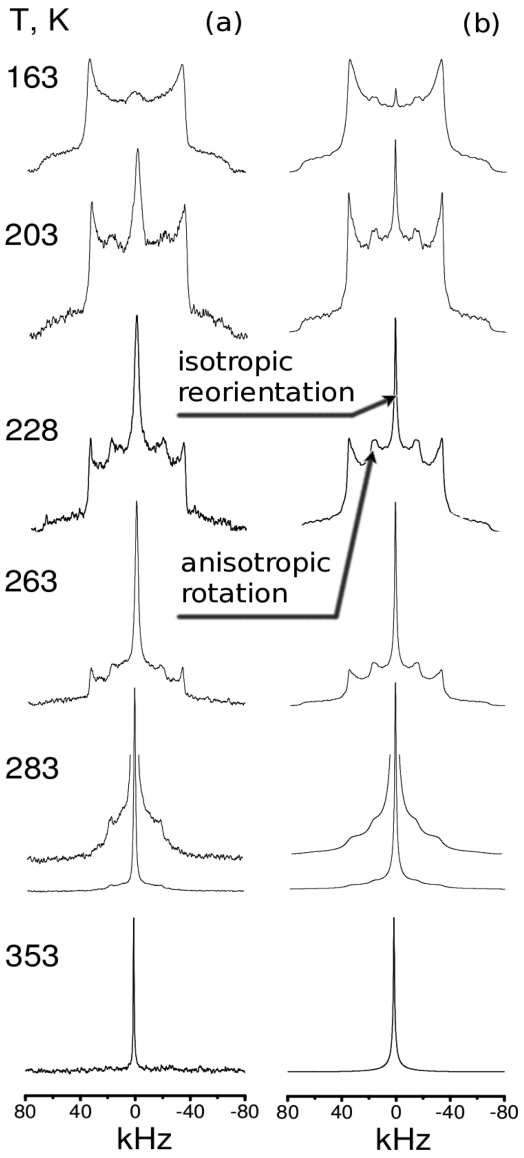


**Figure 7.** $^2$H NMR results: (a) experimental spectra line shape temperature dependence of benzene-$d_6$ adsorbed in MIL-47(V) and (b) simulated spectra.

signals grow, showing a rather peculiar line shape transformation up to the point where both the initial and the narrow anisotropic signals completely disappear leaving only a signal with an isotropic line shape. Such a behavior indicates that above 163 K the benzene molecules in MIL-47(V) are involved into at least two types of rotations: one responsible for the narrow anisotropic signal and the second one for the isotropic one (Figure 7).

The effective interaction constant for the anisotropic signal $Q_2 \approx Q_1/2$ and its shape indicate[30] that the corresponding motion is an anisotropic rotation of benzene around one of its $C_2$ symmetry axes.

The motion responsible for the isotropic signal is more complex: on the one hand, the line shape suggests a molecular reorientation with a symmetry high enough to average the quadrupolar interaction, and on the other hand, it is certainly not an isotropic rotational diffusion, as the latter shows a completely different pattern change in the intermediate exchange regime.[31] The evolution of the line shape indicates a pseudoisotropic jump reorientation, i.e., when the motion is represented by discrete jumps with sufficiently high symmetry.[11,32] Such observations give a general picture of the molecular reorientation. However, to help understanding the $^2$H NMR spectra, the results acquired by the molecular simulations were found to be essential.

The spectrum line shape analysis gives a rather robust picture of the *effective* geometry of the motion.[30] Combined with the analysis of the free-energy landscape, it provides precise information on the dynamic mechanism in play. Indeed, the second (A1 → A2) and the third (A2 → B2) jump sequences (Figure 6d) show that while moving inside the channel, benzene effectively rotates about its $C_2$ axis by $\pi/2$ jumps, thus creating a corkscrew pattern. This motion reflects the anisotropic part of the $^2$H NMR spectra evolution. The motion responsible for the complete averaging of any anisotropic features in the line shape is also in line with the conclusions drawn from the MD trajectories: in ≈0.1% of the jumps, the orientation of the molecular plane gets perpendicular to the channel axis instead of being aligned with it. This motion leads to the turnover of the molecule with respect to the channel axis, thus creating an additional orientation of the benzene inside the channel. When the jump rates are fast enough, the exchange between all possible orientations gives effectively an isotropic averaging of the $^2$H NMR line shape.

Simulations of the spectra (see Supporting Information) show that such a reorientation mechanism fully describes the experimental line shapes (Figure 7). Moreover, the kinetic parameters for each jump−rotation process show a good agreement with the values predicted from MD simulations: the jump exchange between two positions in the same $z$ plane coupled with a $\pi/2$ rotation of the benzene molecule is characterized by $E_2$ = 6 kJ/mol and $k_{20} = 0.6 \times 10^6$ s$^{-1}$, and the motion that involves both a displacement in the same $x,y$ plane and a shift between the $z$ planes also coupled with a $\pi/2$ rotation is characterized by $E_3$ = 13 kJ/mol and $k_{30} = 5 \times 10^6$ s$^{-1}$ (see Figure 8).

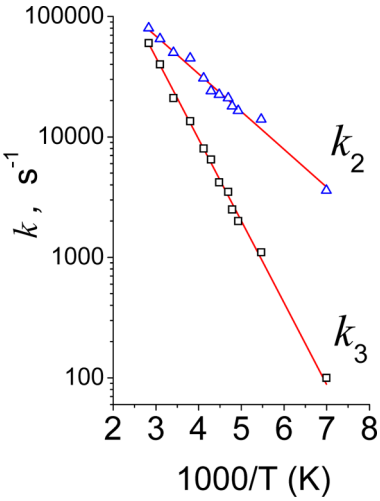


**Figure 8.** Arrhenius plot for the benzene rotational motions observed by $^2$H NMR. $k_2$ is the rate constant for jumps between two positions in the same $z$ plane of the channel coupled with a $\pi/2$ rotation of the benzene molecular plane. $k_3$ is the rate constant for jumps that involve both displacements in the $x,y$ planes and shifts between $z$ planes also coupled with $\pi/2$ rotation. Symbols represent experimental data, and linear fits are given by solid lines.

The small values of the preexponential factors indicate that we monitor rare jumps corresponding to displacements coupled


dx.doi.org/10.1021/jp302995b | J. Phys. Chem. C 2012, 116, 15093−15098

with the reorientation of the benzene molecular plane with respect to the channels axis. This last observation is fully consistent with the MD predictions and explains why these motions cannot be measured by QENS.

## 4. CONCLUSIONS

By combining experimental techniques operating at different time scales with molecular simulations, we were able to fully characterize the peculiar dynamics of benzene confined in MIL-47(V): QENS probes local diffusion at short time scales, and simulations yield diffusivities in agreement with QENS but show in addition less frequent motions that can only be observed by $^2$H NMR. The picture we obtain leads to a molecule that is diffusing along the 1D channels, while randomly rotating by 90° jumps, thus performing a corkscrew motion.

## ■ ASSOCIATED CONTENT

### Supporting Information

Supplementary Figures S1 and S2. $^2$H NMR line shape simulation details. This material is available free of charge via the Internet at http://pubs.acs.org.

## ■ AUTHOR INFORMATION

### Corresponding Author

*E-mail: herve.jobic@ircelyon.univ-lyon1.fr.

### Notes

The authors declare no competing financial interest.

## ■ ACKNOWLEDGMENTS

We thank the Institut Laue-Langevin for neutron beam time. Preparation of the samples for $^2$H NMR experiments by Dr. A. A. Gabrienko is greatly acknowledged. This work was supported by the Russian Foundation for Basic Research (grants RFFI No. 12-03-00316 and No. 09-03-93113) and by the European Community's Seventh Framework Programme (FP7/2007-2013) under grant agreement no. 228862 (MACADEMIA project).

## ■ REFERENCES

(1) Alaerts, L.; Kirschhock, C. E. A.; Maes, M.; van der Veen, M. A.; Finsy, V.; Depla, A.; Martens, J. A.; Baron, G. V.; Jacobs, P. A.; Denayer, J. E. M.; De Vos, D. E. *Angew. Chem., Int. Ed.* **2007**, *46*, 4293.
(2) Finsy, V.; Verelst, H.; Alaerts, L.; De Vos, D.; Jacobs, P. A.; Baron, G. V.; Denayer, J. F. M. *J. Am. Chem. Soc.* **2008**, *130*, 7110.
(3) Alaerts, L.; Maes, M.; Jacobs, P. A.; Denayer, J. F. M.; De Vos, D. E. *Phys. Chem. Chem. Phys.* **2008**, *10*, 2979.
(4) Cychosz, K. A.; Ahmad, R.; Matzger, A. J. *Chem. Sci.* **2010**, *1*, 293.
(5) Li, H.; Eddaoudi, M.; O'Keeffe, M.; Yaghi, O. M. *Nature* **1999**, *402*, 276.
(6) Kitagawa, S.; Kitaura, R.; Noro, S. *Angew. Chem., Int. Ed.* **2004**, *43*, 2334.
(7) Férey, G.; Serre, C.; Devic, T.; Maurin, G.; Jobic, H.; Llewellyn, P. L.; De Weireld, G.; Vimont, A.; Daturi, M.; Chang, J. S. *Chem. Soc. Rev.* **2011**, *40*, 550.
(8) Barthelet, K.; Marrot, J.; Riou, D.; Férey, G. *Angew. Chem., Int. Ed.* **2002**, *41*, 281.
(9) Fitch, A. N.; Jobic, H.; Renouprez, A. *J. Phys. Chem.* **1986**, *90*, 1311.
(10) Auerbach, S. M.; Bull, L. M.; Henson, N. J.; Metiu, H. I.; Cheetham, A. K. *J. Phys. Chem.* **1996**, *100*, 5923.
(11) Geil, B.; Isfort, O.; Boddenberg, B.; Favre, D. E.; Chmelka, B. F.; Fujara, F. *J. Chem. Phys.* **2002**, *116*, 2184.
(12) Jobic, H.; Ramanan, H.; Auerbach, S. M.; Tsapatsis, M.; Fouquet, P. *Microporous Mesoporous Mater.* **2006**, *90*, 307.
(13) Gonzalez, J.; Devi, R. N.; Tunstall, D. P.; Cox, P. A.; Wright, P. A. *Microporous Mesoporous Mater.* **2005**, *84*, 97.
(14) Stallmach, F.; Groger, S.; Kunzel, V.; Karger, J.; Yaghi, O. M.; Hesse, M.; Muller, U. *Angew. Chem., Int. Ed.* **2006**, *45*, 2123.
(15) Amirjalayer, S.; Schmid, R. *Microporous Mesoporous Mater.* **2009**, *125*, 90.
(16) Finsy, V.; Calero, S.; García-Pérez, E.; Merkling, P. J.; Vedts, G.; De Vos, D. E.; Baron, G. V.; Denayer, J. F. M. *Phys. Chem. Chem. Phys.* **2009**, *11*, 3515.
(17) Jobic, H.; Theodorou, D. N. *Microporous Mesoporous Mater.* **2007**, *102*, 21.
(18) Mizuno, M.; Itakura, N.; Endo, K. *Chem. Phys. Lett.* **2005**, *416*, 358.
(19) Antonijevic, S.; Wimperis, S. *J. Magn. Reson.* **2003**, *164*, 343.
(20) Ramsahye, N. A.; Maurin, G.; Bourrelly, S.; Llewellyn, P.; Loiseau, T.; Férey, G. *Phys. Chem. Chem. Phys.* **2007**, *9*, 1059.
(21) Rappe, A. K.; Casewit, C. J.; Colwell, K. S.; Goddard, W. A.; Skiff, W. M. *J. Am. Chem. Soc.* **1992**, *114*, 10024.
(22) Mayo, S. L.; Olafson, B. D.; Goddard, W. A. *J. Phys. Chem.* **1990**, *94*, 8897.
(23) Rai, N.; Siepmann, J. I.; Schultz, N. E.; Ross, R. B. *J. Phys. Chem. B* **2007**, *111*, 15634.
(24) Smith, W.; Forester, T. R. *J. Mol. Graphics* **1996**, *14*, 136.
(25) Frenkel, D.; Smit, B. *Understanding Molecular Simulation*; Academic Press: New York, 1996.
(26) Beerdsen, E.; Smit, B.; Dubbeldam, D. *Phys. Rev. Lett.* **2004**, *93*, 248301.
(27) Jobic, H.; Bée, M.; Renouprez, A. *Surf. Sci.* **1984**, *140*, 307.
(28) Singwi, K. S.; Sjölander, A. *Phys. Rev.* **1960**, *119*, 863.
(29) Ok, J. H.; Vold, R. R.; Vold, R. L.; Etter, M. C. *J. Phys. Chem.* **1989**, *93*, 7618.
(30) Wittebort, R. J.; Olejniczak, E. T.; Griffin, R. G. *J. Chem. Phys.* **1987**, *86*, 5411.
(31) Stocktone, G. W.; Polnaszek, C. F.; Tulloch, A. P.; Hasan, F.; Smith, I. C. P. *Biochemistry* **1976**, *15*, 954.
(32) Spiess, H. W. Rotation of molecules and nuclear spin relaxation. In *NMR Basic Principles and Progress*; Diehl, P., Fluck, E., Kosfeld, R., Eds.; Springer-Verlag: New York, 1978; Vol. *15*; p 55.